CHINESE OPTICS LETTERS

Vol. 21, No. 4 | April 2023

Dual photopatterning of rotational fingerprint superstructures

Jintao Pan (潘锦涛)[1,†], Jiaxin Qian (钱嘉欣)[1,†], Lingling Ma (马玲玲)[1*], Zeyu Wang (王泽宇)[1], Ren Zheng (郑 仁)[1], Ning Wang (王 宁)[1], Bingxiang Li (李炳祥)[2**], and Yanqing Lu (陆延青)[1***]

[1] National Laboratory of Solid State Microstructures, Key Laboratory of Intelligent Optical Sensing and Manipulation, College of Engineering and Applied Sciences, and Collaborative Innovation Center of Advanced Microstructures, Nanjing University, Nanjing 210023, China

[2] College of Electronic and Optical Engineering & College of Flexible Electronics (Future Technology), Nanjing University of Posts and Telecommunications, Nanjing 210023, China

*Corresponding author: malingling@nju.edu.cn

**Corresponding author: bxli@njupt.edu.cn

***Corresponding author: yqlu@nju.edu.cn

Received November 29, 2022 | Accepted January 3, 2023 | Posted Online February 21, 2023

Controlling architecture of hierarchical microstructures in liquid crystals (LCs) plays a crucial role in the development of novel soft-matter-based devices. Chiral LC fingerprints are considered as a prospective candidate for various applications; however, the efficient and real-time command of fingerprint landscapes still needs to be improved. Here, we achieve elaborate rotational fingerprint superstructures via dual photopatterning semifree chiral LC films, which combine the photoalignment technique and a dynamic light patterning process. An intriguing spatial-temporal rotational behavior is presented during the patterning of chiral superstructures. This work opens new avenues for the applications of chiral LCs in soft actuators, sensing, and micromanufacturing.

Keywords: liquid crystal; photoalignment; fingerprints; chiral photoresponsive materials.

DOI: 10.3788/COL202321.041603

1. Introduction

The hierarchical structures from nature have inspired the design of artificial superstructures for centuries, which is crucial for developing novel tools, devices, and systems. Liquid crystals (LCs) are intermediate substances between the liquid state and the solid state, referred to as the fourth state. The orientational ordering of LCs combined with the rod-like molecular shapes of LCs gives rise to intriguing physical anisotropies, which play essential roles in LC applications[1,2]. Generally, the orientational ordering of LCs can be controlled by different boundary geometries[3] and anchoring conditions[4], allowing the formation of diverse structures or superstructures, including topological defects (i.e., focal conic domains[5]). These structures exhibit extraordinary sensitivity to various external stimuli, including light, electric field, heat, force, magnetic field, and so on[6–9]. Thus, there are many degrees of freedom in the way that the structure is coded and the tunability is devised for the design of soft-matter-based devices with innovative functions.

Chirality is ubiquitous in the universe within various scales, from the galaxy to deoxyribonucleic acid in living entities. By combining the "chirality" and the "soft matter" characteristics, chiral LCs (CLCs) are a fertile playground for novel phenomena and functionalities, with various potential applications[10–12], such as distributed feedback lasers, reflective films, dynamic lithography masks, and phase gratings[13–17]. Under appropriate boundary conditions, CLCs can self-assemble into periodic helical superstructures with fingerprint textures, which are believed to have potential for nonmechanical beam steering[14], spectrum scanning[18], particle assembly[19], optical vortices generators[20], lasing[21], anticounterfeiting[22], and lithography[23]. If such fingerprint structures can be rationally designed and dynamically manipulated, new possibilities for the design of novel intelligent devices based on CLC superstructures can be reasonably expected. Fingerprint texture favors antagonistic conditions, and there are different ways to achieve such conditions. For instance, when CLCs are infiltrated in a homeotropic cell, periodic stripes with a lying-helix structure are formed due to the competition between the helical twisted power and the anchoring energy. Another way is to apply a vertical electric field, providing a force to homeotropically align LC molecules, contradicting the intrinsic helical twisted power[18,24]. Hybrid-aligned cells also provide conflicting anchoring conditions for the growth of fingerprints[25,26]. Compared to the above scenarios in cells, ordered fingerprints in semifree films are more

attractive due to the tremendous practical potential of exploiting the surface interactions between the film and air. They can be easily formed on a planarly aligned substrate, utilizing the quasi-homeotropic anchoring from air[27]. Thanks to the unique orientational ordering of CLCs, Feringa *et al.* demonstrated a rotational behavior of microrods mediated by a fingerprint system that is doped with photoresponsive molecular motors[7,28–30]. Li *et al.* reported a series of tunable LC devices based on light-driven molecular switches[31,32]. Despite the progress mentioned above, efficiently and finely controlling fingerprint landscapes forming dynamic and variational chiral superstructures is still challenging.

Here, we achieve the dynamic photopatterning of rotational fingerprints in semifree CLC films. By combining the photoalignment technique and uniform UV light exposure, the spatial rotated fingerprints exhibit temporal rotational behaviors, resulting in diverse fingerprint configurations, such as a radiating structure, a whirlwind pattern, and an Archimedean spiral. In addition, C-shape grating is dynamically created on a unidirectionally photoaligned substrate by utilizing structured light. The combination of photoalignment and photowriting of fingerprints inspires more possibilities for the creation of functional materials and devices.

2. Experimental Materials and Methods

The CLC mixture was composed of nematic E7 (Jiangsu Hecheng Display Technology Co., Ltd., China) and a left-handed chiral molecular motor of ChAD-3c-S (BEAM, U.S.). The concentration of ChAD-3c-S in the CLC mixture was about 0.34% (mass fraction). Confirmed by a differential scanning calorimetry (Mettler-Toledo DSC1 STARe), the operating temperature range is from < -20°C to 58.8°C. Thanks to the two azo linkages, ChAD-3c-S can isomerize from a rod-like trans-form to a bent cis-form structure under UV light irradiation, thus tuning the CLC helical pitch (p). The cis-form of azobenzene is unstable in a natural state, resulting in a reversible transformation when providing ambient temperatures or upon the irradiation of green light. The incorporation of ChAD-3c-S in E7 yields an initial helical twisting power (HTP) of $-42.6\,\mu m^{-1}$ in the dark[33], and the green-light-stabilized HTP is about $-30.7\,\mu m^{-1}$[34].

Photoalignment has become a dominant alignment technique in aligning LCs. The noncontact photoalignment process not only overcomes the prejudicial contamination problems but also could achieve multidomain and high-resolution alignment. Here, a 0.3% solution of sulfonic azo dye SD1 (Dai-Nippon Ink and Chemicals, Japan) in dimethylformamide (DMF) was used as a photoalignment agent. SD1 molecules tend to reorient their long axes perpendicular to the incident linear polarization of UV or blue light to minimize photon absorption. The resulting azimuthal anchoring energy is over $10^{-4}\,J/m^2$, which is comparable to that of the rubbed polyimide film[35]. By providing regular alignment, the LC molecules adjacent to the alignment layer will be guided to align in an orderly manner, subsequently inducing the organization of bulk LCs due to the long-range orientational ordering.

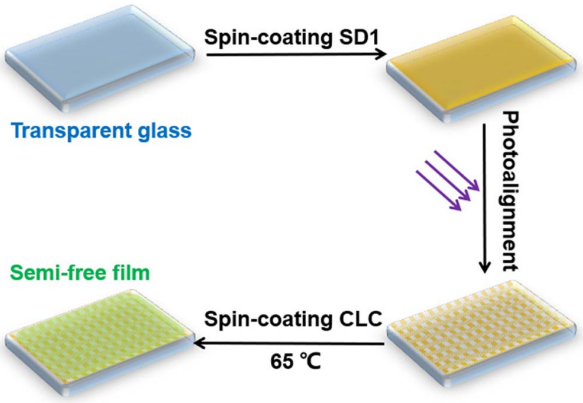

Fig. 1. Preparation procedure of fingerprints.

As shown in Fig. 1, transparent glass substrates (1.5 cm × 2 cm) were ultrasonically bathed, UV-ozone cleaned, and then spin-coated with SD1. After curing at 100°C for 10 min, the substrates were placed at the image plane of the digital micromirror device (DMD)-based microlithography system to record the designed alignment pattern. Afterward, the CLC mixture was spread onto the substrates at 65°C and spin-coated at 1000 r/min for 30 s to fabricate the semifree CLC film. Then the samples were observed under a cross-polarized optical microscope (POM) (Nikon Eclipse 50i Pol, Tokyo, Japan). Noticeably, the light source from the microscope was to be kept as weak as possible. The dynamic photopatterning process was performed with a 365 nm LED. The light intensity for constant UV light stimulation is $\sim 100\,\mu W/cm^2$. The intensity of the structural light field is in the range of 10–140 $\mu W/cm^2$. The green-light exposure process was carried out with an LED light source at 530 nm with an intensity of $1.0\,mW/cm^2$.

3. Experimental Results

3.1. Hierarchical fingerprint superstructures

After the photoresponsive CLC is spin-coated onto a unidirectionally aligned substrate, uniform fingerprint stripes are formed [Fig. 2(a)]. The stripe period is about 7.1 μm. According to Baudry's model[25], such a structure comprises two parts. In the first part, planar helical layers develop from the substrate and occupy the bulk of the film with helical axes perpendicular to substrates [Figs. 2(b) and 2(d)]. The intrinsic periodic helical structure is regarded as the first hierarchy. Due to the competition between the internal HTP and the external antagonistic anchoring energy (substrate, planar anchoring; air, homeotropic anchoring), helical layers near the air/LC interface distort periodically. Besides the helical organization, directors gradually tilt from 0° to 90° (violet line indicated) and periodically twirl by $\delta(x)$ around the cone axis [red line indicated, Fig. 2(c)]. Due to the continuity of LCs, the cone angle $\gamma(z)$ reaches the maximum in the middle of the second part

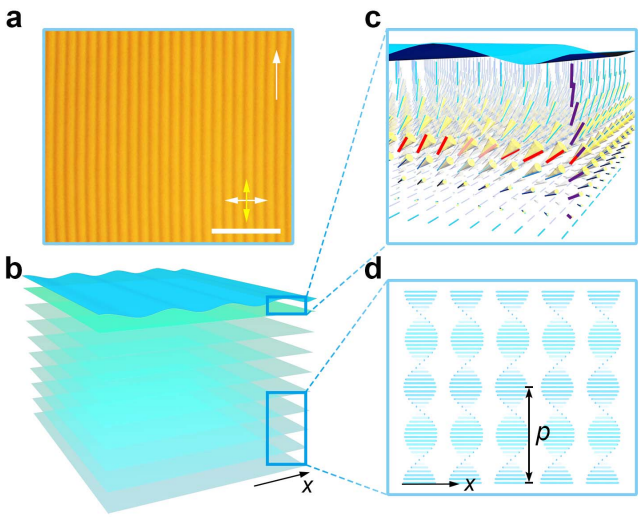

Fig. 2. Fingerprints with hierarchical helix structures. (a) Polarized optical microscope textures of unidirectionally aligned fingerprints; scale bar, 50 μm; (b)–(d) schematics of the hierarchical helical structure, planar helices with helical axes perpendicular to substrates, and the self-adapted distorted helical structure near the air–film interface; the distance between two adjacent layers equals half a pitch.

and gradually vanishes when approaching the two interfaces. The director field is assumed to be translationally invariant in *y*, thus resulting in a periodic variation of refractive index, corresponding to the alternating bright and dark stripes in the texture. This configuration is regarded as the second hierarchy. Due to the photoresponsive property of CLCs, the initial direction of fingerprint stripes is related to the alignment, and the external light field can further tune it.

As mentioned above, the photoalignment technique can spatially program the local orientational ordering of LC directors, which provides a valuable tool to introduce another hierarchy to the CLC fingerprint configuration. Here, we design binary and continuous periodic alignment patterns, as shown in Figs. 3(a) and 3(b). The included angle of alignment in adjacent regions is about 100° [Fig. 3(a)]. Consequently, a zigzag fingerprint pattern in line with expectations is formed, a common and important phenomenon in nature serving multiple purposes. The direction of fingerprint stripes has a unified fixed angle relative to the underlying alignment, verifying the periodic photoalignment-induced third hierarchy. In addition, fingerprint stripes can continuously change their directions by implementing a continuously varied alignment. As shown in Fig. 3(b), a periodic C-shape fingerprint pattern is generated with Burgers vector dislocations, which are inevitable and play essential roles in the growth of the fingerprint landscape. Thus, more complex and functional fingerprint textures can be achieved by rationally designing the alignment structures.

3.2. Dual photopatterning of rotational fingerprints

By taking advantage of the stimuli-responsive capability of LCs, the spatial-temporal photopatterning of rotational fingerprints

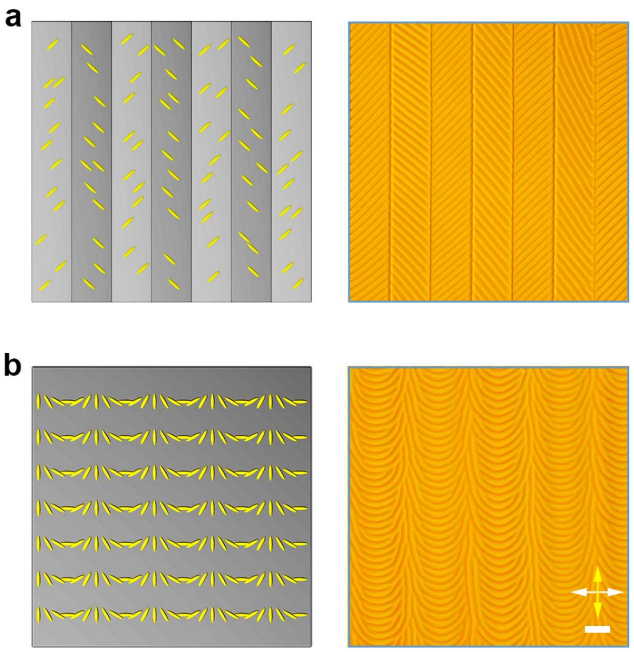

Fig. 3. Photopatterned hierarchical fingerprints. (a) Binary periodic alignment and periodic zigzag fingerprint pattern; (b) continuous periodic alignment and C-shaped fingerprint superstructure; scale bar, 50 μm.

is also demonstrated. Here, we set a radially aligned substrate with anchoring direction rotating around the pole. After the CLC is spin-coated, radial fingerprint stripes occur around a central singularity where the alignment cannot be defined [Fig. 4(a)]. After the sample is exposed to uniform UV light, the spatially rotated fingerprints exhibit temporally rotational behaviors. All the stripes synchronously rotate counterclockwise, presenting a radiating structure, a whirlwind pattern, and an Archimedean spiral successively. This phenomenon is because of the light-induced isomerization of the chiral molecular switch, which decreases the HTP and subsequently modifies the stripe configuration. Finally, the stripes disappear due to insufficient HTP to reconcile the antagonistic anchoring energy. The above dynamic photopatterning process is reversible when the sample is under a high ambient temperature or upon green-light irradiation [Fig. 4(b)].

Furthermore, the structured light field can add another dimension for the photopatterning of complex fingerprint superstructures, which has attracted more attention in recent years in functional pattern formation. Here, we select a simple asymmetric light field with a linear intensity gradient as a demonstration [Fig. 5(a)]. In this case, unidirectional stripes under the exposure region rotate in the same direction but not in synchronization. The rotational speed of regional fingerprints is determined by the exposure intensity. Stripe domains under bright light show an intense rotational behavior compared to dim light. As shown in Fig. 5(b), the continuous rotation of stripes leads to the formation of periodic C-shaped fingerprints observed between crossed polarizers. During the dynamic photopatterning, the total rotational angle reaches about 650°,

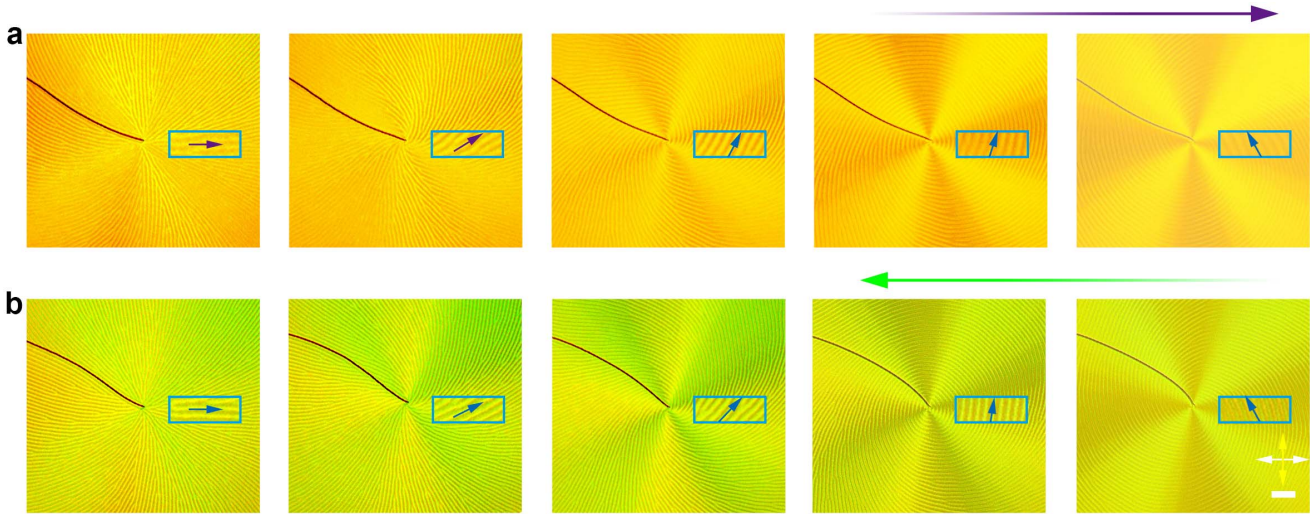

Fig. 4. Dual photopatterning of rotational fingerprints. (a) Changing process from a radiating structure to Archimedean spiral during the uniform UV light exposure; (b) changing process from an Archimedean spiral to radiating structure during the uniform green-light exposure; scale bar, 50 μm.

corresponding to the periodicity of the formed fingerprint pattern, and the stripe period is increased from 5.9 to 9.7 μm [Fig. 5(c)].

4. Discussions and Conclusions

So far, we have achieved dual photopatterning of rotational fingerprint superstructures in a photoresponsive CLC system. On the one hand, a spatial-temporal varied rotational fingerprint pattern is realized by combining the structured photoalignment and the uniform light exposure. Consequently, versatile stripe configurations in different formations are obtained, including a radiating structure, a whirlwind pattern, and an Archimedean spiral. On the other hand, we proposed the cooperation of uniform photoalignment and direct-writing of structured light to efficiently dictate high-resolution multidomain fingerprint superstructures, such as C-shaped fingerprints, as shown in Figs. 3(b) and 5(b). With their strong alliance, we can not only preprogram the primitive superstructures but also

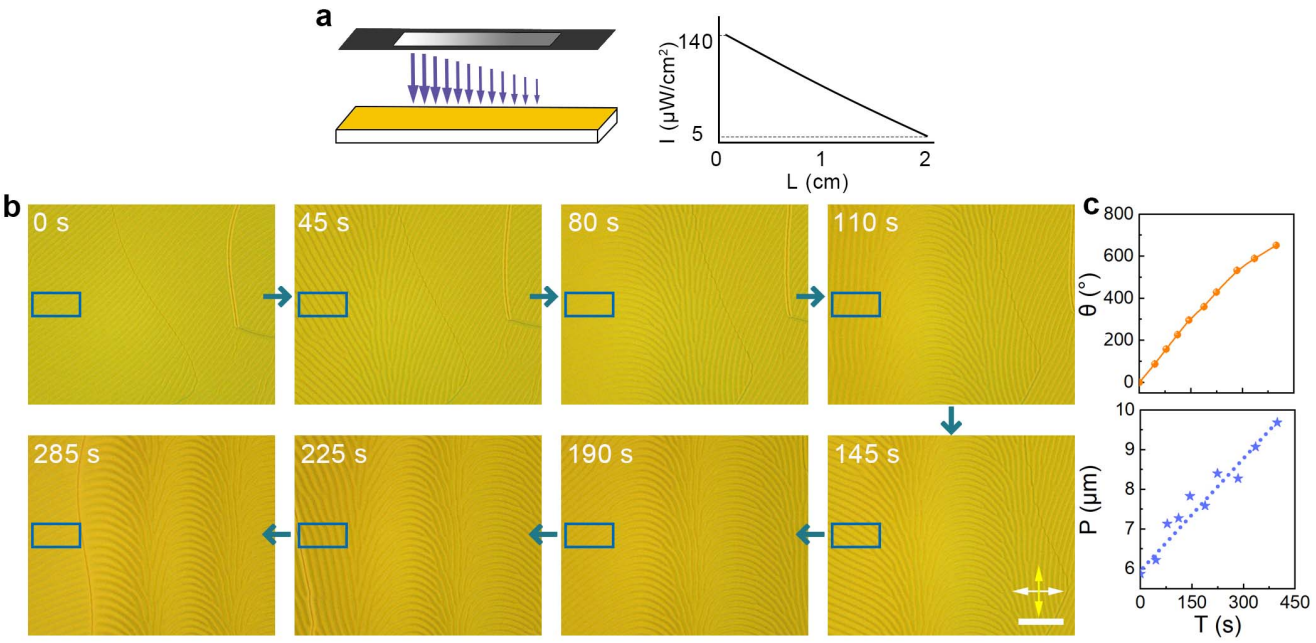

Fig. 5. Photopatterning of rotational fingerprint superstructures. (a) Schematic of structured light exposure process. The intensity of the 365-nm light source is 10–140 μW/cm^2, and the lengths of purple arrows indicate the varied intensity of light. (b) Evolution of the fingerprint superstructure during the irradiation; scale bar, 50 μm; (c) relationships between the period of fingerprint stripes, rotational angle, and the exposure time.

dictate regional fingerprints in real time to form desired configurations. These photopatterning processes show an easy procedure, noncontact operation, and remote and reversible control. In addition, the dynamic photowriting approach requires incoherent light sources (an LED or a halogen lamp) with a relatively weak intensity of about 100 $\mu W/cm^2$, which significantly avoids light damage to the sample[36]. Thanks to the intrinsic self-assembly of CLCs, the programmable fingerprint structures are simple to fabricate, reconfigurable, cost-efficient, and easy to miniaturize.

As mentioned above, fingerprints formed in semifree films with unique anisotropic interfaces have several strengths. With such dual photopatterning, LCs' elasticity field changes dynamically, which can be exploited to manipulate functional objects or guide the movement of living motile cells. Apart from the micromanipulation application, we also expect that they have specific applications in light-field control, such as programmable beam steering elements, rewritable beam focusing devices, and on-demand vortex generators, based on chiral fingerprint superstructures. Recently, the ferroelectric nematic mesophase, expected since at least 1916, has been uncovered[37]. This phase possesses ferroelectricity, huge low-frequency dielectric constants, and spontaneous polar ordering[38,39]. A series of studies have reported self-assembled helical polar structures by doping chiral additives, which will open up new opportunities for polar fingerprints and introduce new physical properties to fingerprints, such as electro-optic, electromechanical, and nonlinear optical effects.

In conclusion, we demonstrate dual photopatterning and exploit its potential of dynamically dictating rotational fingerprint superstructures. First, we clarify the hierarchy of fingerprint superstructures. Then hierarchical superstructures with periodic fingerprint textures are easily fabricated using the photoalignment technique. Under stimulating light, photoaligned radial fingerprints are continuously and reversibly deformed into different configurations, which are expected to have significant promise in optoelectronic applications. Moreover, structured light is utilized to achieve a dynamic photopatterning of a similar C-shaped fingerprint superstructure. Such systems are performed with self-organized photoresponsive microstructures, which are instructive in the design of intelligent materials. This work provides a clearer picture of the hierarchical fingerprint superstructure and may trigger new directions for future developments of fingerprint-based optical elements, micromanipulation, integrated sensors, and anticounterfeiting systems.

Acknowledgement

This work was supported by the National Key Research and Development Program of China (Nos. 2021YFA1202000 and 2022YFA1405000), the National Natural Science Foundation of China (No. 52003115), the Natural Science Foundation of Jiangsu Province, Major Project (No. BK20212004), and the Natural Science Foundation of Jiangsu Province (No. BK20200320). L. Ma gratefully acknowledges the support of Xiaomi Young Scholar program.

†These authors contributed equally to this work.

References

1. L.-L. Ma, C.-Y. Li, J.-T. Pan, Y.-E. Ji, C. Jiang, R. Zheng, Z.-Y. Wang, Y. Wang, B.-X. Li, and Y.-Q. Lu, "Self-assembled liquid crystal architectures for soft matter photonics," Light Sci. Appl. **11**, 270 (2022).
2. Y. Gao, W. Ding, and J. Lu, "Templated twist structure liquid crystals and photonic applications," Polymers **14**, 2455 (2022).
3. A. Honglawan, D. A. Beller, M. Cavallaro, R. D. Kamien, K. J. Stebe, and S. Yang, "Topographically induced hierarchical assembly and geometrical transformation of focal conic domain arrays in smectic liquid crystals," Proc. Natl. Acad. Sci. USA **110**, 34 (2013).
4. L.-L. Ma, M.-J. Tang, W. Hu, Z.-Q. Cui, S.-J. Ge, P. Chen, L.-J. Chen, H. Qian, L.-F. Chi, and Y.-Q. Lu, "Smectic layer origami via preprogrammed photoalignment," Adv. Mater. **29**, 1606671 (2017).
5. L.-L. Ma, S.-B. Wu, W. Hu, C. Liu, P. Chen, H. Qian, Y. Wang, L. Chi, and Y.-Q. Lu, "Self-assembled asymmetric microlenses for four-dimensional visual imaging," ACS Nano **13**, 13709 (2019).
6. H. Sun, Z. Xie, C. Ju, X. Hu, D. Yuan, W. Zhao, L. Shui, and G. Zhou, "Dye-doped electrically smart windows based on polymer-stabilized liquid crystal," Polymers **11**, 694 (2019).
7. N. A. Razali and Z. Jamain, "Liquid crystals investigation behavior on azo-based compounds: a review," Polymers **13**, 3462 (2021).
8. B. Liu, C. L. Yuan, H. L. Hu, H. Wang, Y. W. Zhu, P. Z. Sun, Z. Y. Li, Z. G. Zheng, and Q. Li, "Dynamically actuated soft heliconical architecture via frequency of electric fields," Nat. Commun. **13**, 2712 (2022).
9. Z. Song, Z. Li, X. Shang, C. Li, L. Ma, Y. Lu, and B. Li, "Electrically switchable structural patterns and diffractions in a dual frequency nematic liquid crystal," Chin. Opt. Lett. **21**, 010501 (2023).
10. Y. Cao, L. Chong, K.-H. Wu, L.-Q. You, S.-S. Li, and L.-J. Chen, "Dynamic coloration of polymerized cholesteric liquid crystal networks by infiltrating organic compounds," Chin. Opt. Lett. **20**, 091602 (2022).
11. L. Ma, C. Li, L. Sun, Z. Song, Y. Lu, and B. Li, "Submicrosecond electro-optical switching of one-dimensional soft photonic crystals," Photon. Res. **10**, 786 (2022).
12. T. Zhan, J. Xiong, J. Zou, and S.-T. Wu, "Multifocal displays: review and prospect," PhotoniX **1**, 10 (2020).
13. M. Mitov, "Cholesteric liquid crystals with a broad light reflection band," Adv. Mater. **24**, 6260 (2012).
14. A. Ryabchun and A. Bobrovsky, "Cholesteric liquid crystal materials for tunable diffractive optics," Adv. Opt. Mater. **6**, 1800335 (2018).
15. S. Cho, H. Yoshida, and M. Ozaki, "Emission direction-tunable liquid crystal laser," Adv. Opt. Mater. **8**, 2000375 (2020).
16. P. Chen, L.-L. Ma, W. Duan, J. Chen, S.-J. Ge, Z.-H. Zhu, M.-J. Tang, R. Xu, W. Gao, T. Li, W. Hu, and Y.-Q. Lu, "Digitalizing self-assembled chiral superstructures for optical vortex processing," Adv. Mater. **30**, 1705865 (2018).
17. X. Zhang, Y. Xu, C. Valenzuela, X. Zhang, L. Wang, W. Feng, and Q. Li, "Liquid crystal-templated chiral nanomaterials: from chiral plasmonics to circularly polarized luminescence," Light Sci. Appl. **11**, 223 (2022).
18. H. C. Jau, Y. Li, C. C. Li, C. W. Chen, C. T. Wang, H. K. Bisoyi, T. H. Lin, T. J. Bunning, and Q. Li, "Light-driven wide-range nonmechanical beam steering and spectrum scanning based on a self-organized liquid crystal grating enabled by a chiral molecular switch," Adv. Opt. Mater. **3**, 166 (2015).
19. L.-L. Ma, C. Liu, S.-B. Wu, P. Chen, Q.-M. Chen, J.-X. Qian, S.-J. Ge, Y.-H. Wu, W. Hu, and Y.-Q. Lu, "Programmable self-propelling actuators enabled by a dynamic helical medium," Sci. Adv. **7**, eabh3505 (2021).
20. D. Voloschenko and O. D. Lavrentovich, "Optical vortices generated by dislocations in a cholesteric liquid crystal," Opt. Lett. **25**, 317 (2000).
21. W. Huang, C.-L. Yuan, D. Shen, and Z.-G. Zheng, "Dynamically manipulated lasing enabled by a reconfigured fingerprint texture of a cholesteric self-organized superstructure," J. Mater. Chem. C **5**, 6923 (2017).

22. W.-S. Li, Y. Shen, Z.-J. Chen, Q. Cui, S.-S. Li, and L.-J. Chen, "Demonstration of patterned polymer-stabilized cholesteric liquid crystal textures for anti-counterfeiting two-dimensional barcodes," Appl. Opt. **56**, 601 (2017).
23. H. S. Jeong, Y. H. Kim, J. S. Lee, J. H. Kim, M. Srinivasarao, and H. T. Jung, "Chiral nematic fluids as masks for lithography," Adv. Mater. **24**, 381 (2012).
24. L.-L. Ma, S.-S. Li, W.-S. Li, W. Ji, B. Luo, Z.-G. Zheng, Z.-P. Cai, V. Chigrinov, Y.-Q. Lu, W. Hu, and L.-J. Chen, "Rationally designed dynamic superstructures enabled by photoaligning cholesteric liquid crystals," Adv. Opt. Mater. **3**, 1691 (2015).
25. J. Baudry, M. Brazovskaia, L. Lejcek, P. Oswald, and S. Pirkl, "Arch-texture in cholesteric liquid crystals," Liq. Cryst. **21**, 893 (1996).
26. A. Ryabchun, A. Bobrovsky, J. Stumpe, and V. Shibaev, "Rotatable diffraction gratings based on cholesteric liquid crystals with phototunable helix pitch," Adv. Opt. Mater. **3**, 1273 (2015).
27. L.-L. Ma, W. Duan, M.-J. Tang, L.-J. Chen, X. Liang, Y.-Q. Lu, and W. Hu, "Light-driven rotation and pitch tuning of self-organized cholesteric gratings formed in a semi-free film," Polymers **9**, 295 (2017).
28. W. R. Browne and B. L. Feringa, "Making molecular machines work," Nat. Nanotechnol. **1**, 25 (2006).
29. R. Eelkema, M. M. Pollard, J. Vicario, N. Katsonis, B. S. Ramon, C. W. Bastiaansen, D. J. Broer, and B. L. Feringa, "Molecular machines: nanomotor rotates microscale objects," Nature **440**, 163 (2006).
30. R. Eelkema, M. M. Pollard, N. Katsonis, J. Vicario, D. J. Broer, and B. L. Feringa, "Rotational reorganization of doped cholesteric liquid crystalline films," J. Am. Chem. Soc. **128**, 14397 (2006).
31. J. Li, H. K. Bisoyi, S. Lin, J. Guo, and Q. Li, "1,2-dithienyldicyanoethene-based, visible-light-driven, chiral fluorescent molecular switch: rewritable multimodal photonic devices," Angew. Chem. Int. Ed. **58**, 16052 (2019).
32. J. Yang, X. Zhang, X. Zhang, L. Wang, W. Feng, and Q. Li, "Beyond the visible: bioinspired infrared adaptive materials," Adv. Mater. **33**, 2004754 (2021).
33. C.-W. Chen, C.-C. Li, H.-C. Jau, C.-H. Lee, C.-T. Wang, and T.-H. Lin, "Bistable light-driven π phase switching using a twisted nematic liquid crystal film," Opt. Express **22**, 12133 (2014).
34. K. C. Huang, Y. C. Hsiao, I. V. Timofeev, V. Y. Zyryanov, and W. Lee, "Photo-manipulated photonic bandgap devices based on optically tristable chiral-tilted homeotropic nematic liquid crystal," Opt. Express **24**, 25019 (2016).
35. H. Wu, W. Hu, H.-C. Hu, X.-W. Lin, G. Zhu, J.-W. Choi, V. G. Chigrinov, and Y.-Q. Lu, "Arbitrary photo-patterning in liquid crystal alignments using DMD based lithography system," Opt. Express **20**, 16684 (2012).
36. M. Yada, J. Yamamoto, and H. Yokoyama, "Direct observation of anisotropic interparticle forces in nematic colloids with optical tweezers," Phys. Rev. Lett. **92**, 185501 (2004).
37. X. Chen, E. Korblova, D. Dong, X. Wei, R. Shao, L. Radzihovsky, M. A. Glaser, J. E. Maclennan, D. Bedrov, D. M. Walba, and N. A. Clark, "First-principles experimental demonstration of ferroelectricity in a thermotropic nematic liquid crystal: polar domains and striking electro-optics," Proc. Natl. Acad. Sci. USA **117**, 14021 (2020).
38. X. Zhao, J. Zhou, J. Li, J. Kougo, Z. Wan, M. Huang, and S. Aya, "Spontaneous helielectric nematic liquid crystals: electric analog to helimagnets," Proc. Natl. Acad. Sci. USA **118**, e2111101118 (2021).
39. X. Zhao, H. Long, H. Xu, J. Kougo, R. Xia, J. Li, M. Huang, and S. Aya, "Nontrivial phase matching in helielectric polarization helices: universal phase matching theory, validation, and electric switching," Proc. Natl. Acad. Sci. USA **119**, e2205636119 (2022).